Submillimeter 3-D laser radar for Space Shuttle tile inspection

J.F. Andersen [a], J. Busck [ab] and H. Heiselberg [a].
[a]Danish Defense Research Establishment, Ryvangs Alle 1, DK-2100 Copenhagen, Denmark.
[b]Technical University of Denmark, Ørsteds Plads, bldg. 349, DK-2800 Kgs. Lyngby, Denmark.

ABSTRACT

A laser radar system based on a green pulsed laser triggering a picosecond camera is described. It has depth accuracy down to 0.2 mm and can therefore do very high accuracy 3-D imaging. The data recording takes only a few seconds, and it works at ranges up to several hundred meters with submillimeter accuracy. Applications to surface tile inspection of a miniature space shuttle are shown and the resolution of cracks and defects is demonstrated. Specific examples are shown that are relevant for the planned laser radar inspections at close range from the space shuttle boom and the longer range survey from the International Space Station.

Keywords: Laser radar, 3-D imaging and survey, gated viewing, space shuttle tile inspection.

1. INTRODUCTION

The Columbia disaster during reentry was according to the accident investigation board caused by a piece of foam from the external tanks striking and damaging the reinforced carbon-carbon tiles on the leading edge of its left wing during launch. NASA has therefore developed a spaceborn scanning laser radar system for inspecting the space shuttle thermal protection shield in 3-D in order to detect cracks or defects in tiles or missing pieces [1-4]. The resolution of these laser radar systems is down to 6 *mm*. The laser radar system can be attached to the extended boom in order to scan below the shuttle. Another system will be placed on the International Space Station (ISS) used for scanning the space shuttle before docking. A number of requirements must be met. Most importantly, the damage threshold for the thermal protecting tiles with the highest heat and pressure loads is 6×6 mm^2 (0.25×0.25 $inch^2$). This threshold has been set as requirement for a candidate 3-D laser radar system. It is shown that the gated viewing 3-D laser radar presented here is well capable of meeting this requirement at ranges up to several hundred meters.

Range information is useful for identifying objects in addition to ordinary reflectivity images. 3-D laser radar imaging has been greatly improved in the last decade by technologies based on gated viewing laser radars [5-7], scanning streak tube imaging laser radars [8-10], avalanche photodiode detector [11] and array [12], time-of-flight phase detectors [13], self-mixing detectors [14], single pulse flash laser radars [15], etc. The techniques vary in range accuracy, resolution, recording time, spectral coverage, etc., with a clear trend towards faster and better accuracy and resolution. Typical accuracies of laser range finders are a few centimeters at distances up to 100 *m* [16].

A number of applications of these systems have been demonstrated such as gated viewing through camouflage and foliage. Backscatter from fog, smoke and water can be reduced thus improving image contrast and viewing in general. It is now possible to do fast 3-D imaging with high accuracy, which greatly improves recognition and identification. An example of such high accuracy 3-D imaging was recently demonstrated for face recognition and person identification at ranges up to 500 *m* [7].

The purpose of this work is to demonstrate sub millimeter accuracy in 3-D with an upgraded version of our laser radar. The system will be described in section 2 together with the 3-D imaging technique. The distance accuracy is shown in section 3 and its detailed dependence on laser power, camera gain, target reflection and range, gate time and step is discussed. Finally, we

demonstrate the depth accuracy on standard targets including a model of a space shuttle both at close range as from the space shuttle boom and at a longer range as in a survey from the ISS. Applications of our system to surface scanning and inspection, its duration and accuracy, etc. are mentioned in the summary.

2. LASER RADAR PROTOTYPE AND 3-D METHOD

Our laser radar prototype system has been described in detail in Refs. [6,7]. It consists of a picosecond pulsed green laser triggering a fast intensified camera. The laser is a 532 *nm* diode pumped solid-state dual-chip Nanolaser. Pulse width is less than 500 *ps*, pulse energy of 4.3 μJ, pulse repetition frequency (PRF) of 32.4 *kHz*, average power of 140 *mW*, and peak power of 8.6 *kW*. Beam divergence is 1.5 *mrad,* which is passed through optics adjusted to the desired field of illumination. From the laser a single trigger line is connected directly to the CCD camera so that the timing of each individual pulse is known to picosecond accuracy. The camera contains an intensified micro channel plate (MCP) of diameter 25 *mm*. The CCD consists of 752×582 detector elements. The size of the CCD is 6×4.5 mm^2. Camera shutter is controlled externally by a trigger signal from the laser for each individual pulse. The spectral response of the detector is 110-800 *nm*. Minimum camera gate time is t_{gate} = 200 *ps*. In the upgraded version both camera gate and delay step t_{delay} can be varied in steps in excess of Δt = 10 *ps*. For high accuracy imaging at short and intermediate distances, we use 100-500 *mm* optics, whereas at long distances we use a 14-inch Celestron telescope with focal length of 4 *m*, (Fig. 1). Daylight is much reduced by the small field of view and short gating time, and is further reduced by inserting a narrow filter with a bandwidth of 530-540 *nm*.

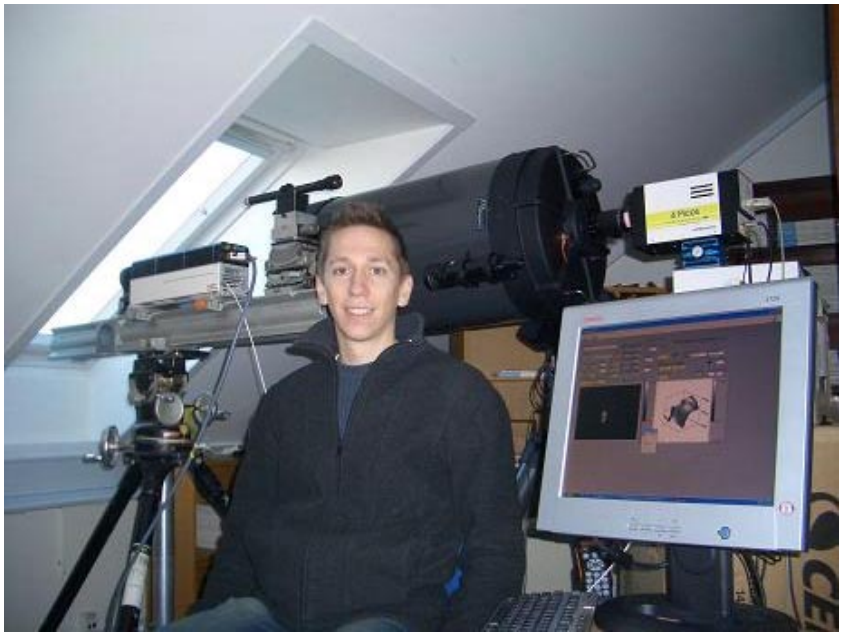

Fig. 1. In front the first author and screen displaying the 3-D software. Behind the picosecond laser (left), 14-inch telescope (middle) and camera (right) are seen.

The 3-D images are built up by taking a series of image frames I_i increasing the delay time: $t_i = t_{i-1} + \Delta t$, for each frame step i = 1, 2, ..., n. Here the number of frames is typically n = *50-500*, depending on the range we want to cover around the target.

The total intensity in each pixel is the sum over frames

$$I(x,y) = \sum_{i=1}^{n} I_i(x,y), \tag{1}$$

where $I_i(x,y)$ is the intensity in the i'th frame in pixel (x,y), see Fig. 2.

The distance z to a target point in any pixel is then

$$z(x,y) = \frac{c}{2I}\sum_{i=1}^{n} t_i I_i = \frac{c}{2}\left[t_0 + \frac{\Delta t}{I}\sum_{i=1}^{n} i\, I_i \right] \tag{2}$$

where Δt is the delay step and t_0 is the initial delay time. Both are preset in the laser-camera triggering. The speed of light is c = 0.3 *mm/ps*. The pixel coordinates (x,y) are related to the 752×582 pixel numbers by multiplying by the focal length and range and dividing by detector size. We refer to Refs. [6,7] for further details on background subtraction, threshold settings, saturation effects, etc.

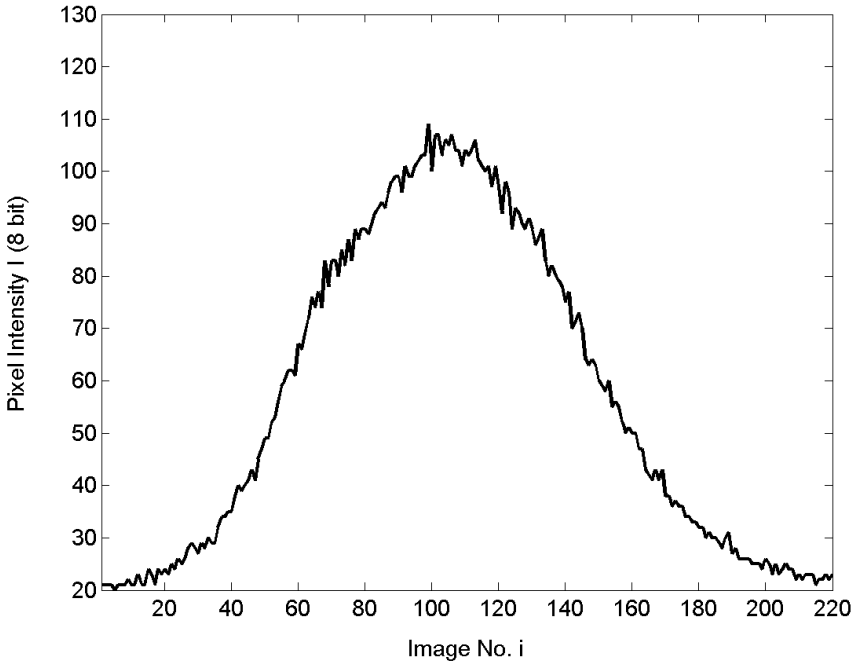

Fig. 2. Experimental values I_i in one pixel versus image number for delay step Δt = 10 *ps*. Gate time fixed at t_{gate} = 500 *ps*. The range is 8 *m*.

An important quantity is the variance in the return time

$$\sigma^2 = < t_i^2 > - < t_i >^2 \cong \sigma_{pulse}^2 + \sigma_{gate}^2 , \tag{4}$$

As shown in [6] the variance is the sum of the variance of the laser pulse time plus the variance of the camera gate time (each are around (500 *ps*)^2 for our system). σ / Δt is also the width of the distribution of Fig. 2. If the camera gate is open for a time t_{gate} and opens and shuts fast, then the root-mean-square or standard deviation of the gate time is $\sigma_{gate} = t_{gate}/\sqrt{12}$. Although the camera gate is not sharp, the variance can be described approximately by inserting such a sharp gate in Eq. (4) as shown in Fig. 3.

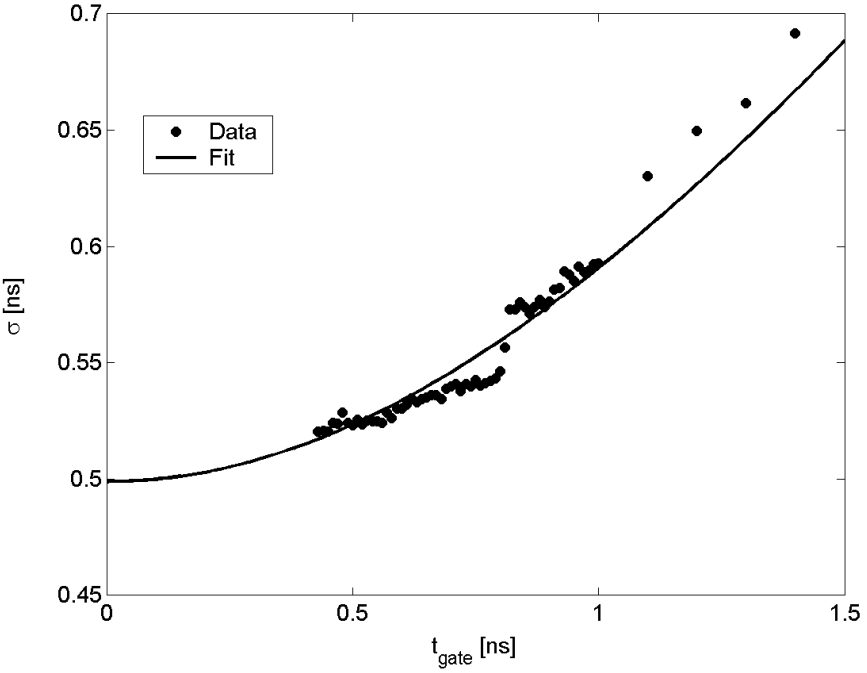

Fig. 3. The standard deviation σ vs. gate time t_{gate}. Points are measurement as taken from data similar to Fig. 2 for each t_{gate} (see text). The curve is Eq. (4) with σ_{pulse} = 0.5 *ns* and assuming a sharp camera gate function $\sigma_{gate} = t_{gate} / \sqrt{12}$.

3. Distance accuracy and 3-D resolution

The accuracy and resolution in distance are important quantities for 3-D imaging. The resolution is determined by the width $\sim c\sigma$, which again is related to the width of the intensity versus frame distribution in Fig. 2 as: $\sqrt{(\langle i^2\rangle - \langle i\rangle^2)} = \sigma/\Delta t$. It is important to realize, however, that the distance accuracy Δz is much smaller because we can step by a much smaller time Δt and sum over a large number of frames. Thereby the noise squared is reduced by a factor proportional to the number of frames running over the pulse, i.e. $\sim\sigma / \Delta t$. The resulting distance accuracy thus scales as $\Delta z \sim \sqrt{\sigma\, \Delta t}$ as described in detail in Ref. [6] (see also Fig. 4). The coefficient of proportionality is a detector constant that varies with the camera gain. Defining the optimal signal-to-noise ratio as SNR_0 we find

$$\Delta z \approx 10^{-2}\, c \sqrt{\sigma\, \Delta t}\, \frac{SNR_0}{SNR}. \qquad (5)$$

The numerical prefactor is a measured detector constant. At long distances, poor target reflectivity or in turbid media (see, e.g. [17]) less pulsed laser light returns to the camera and we must increase the gain. The *SNR* is then found to decrease by up to an order of magnitude for our camera resulting in poorer distance accuracy. Using larger optics or a more powerful laser reduces the need for gain.

The resulting distance accuracy in each pixel is shown in Fig. 4 as function of the delay step Δt. By illuminating a white board we measure the distance z to each pixel. Its average $\langle z\rangle$ is the same and Δz is measured as the RMS of the distance averaged over pixels: $\Delta z = \sqrt{(\langle z^2\rangle - \langle z\rangle^2)}$. The measured distance accuracy is well described by the square root prediction of Eq. (5). The

minimum value or, equivalently, the highest distance accuracy is $\Delta z \sim 0.2$ *mm* under optimal conditions and minimum step time $\Delta t = 10$ *ps*. Inserting this value and $\sigma = 500$ *ps* in Eq. (5) also gives $\Delta z \sim 0.2$ *mm*. This high accuracy traces back to the high sensitive MCP detector, the narrow pulses, fast and jitter-free camera and the summation of many pulses in each frame. Also each frame I_i contains a large number of laser pulses (~650) due to the high laser PRF resulting in a large SNR_0. The large sum of pulses also makes each frame practically speckle free. This accuracy is considerably better than reported in previous publications [6-8] and is mainly due to a camera upgrade where Δt was reduced by an order of magnitude to 10 *ps*.

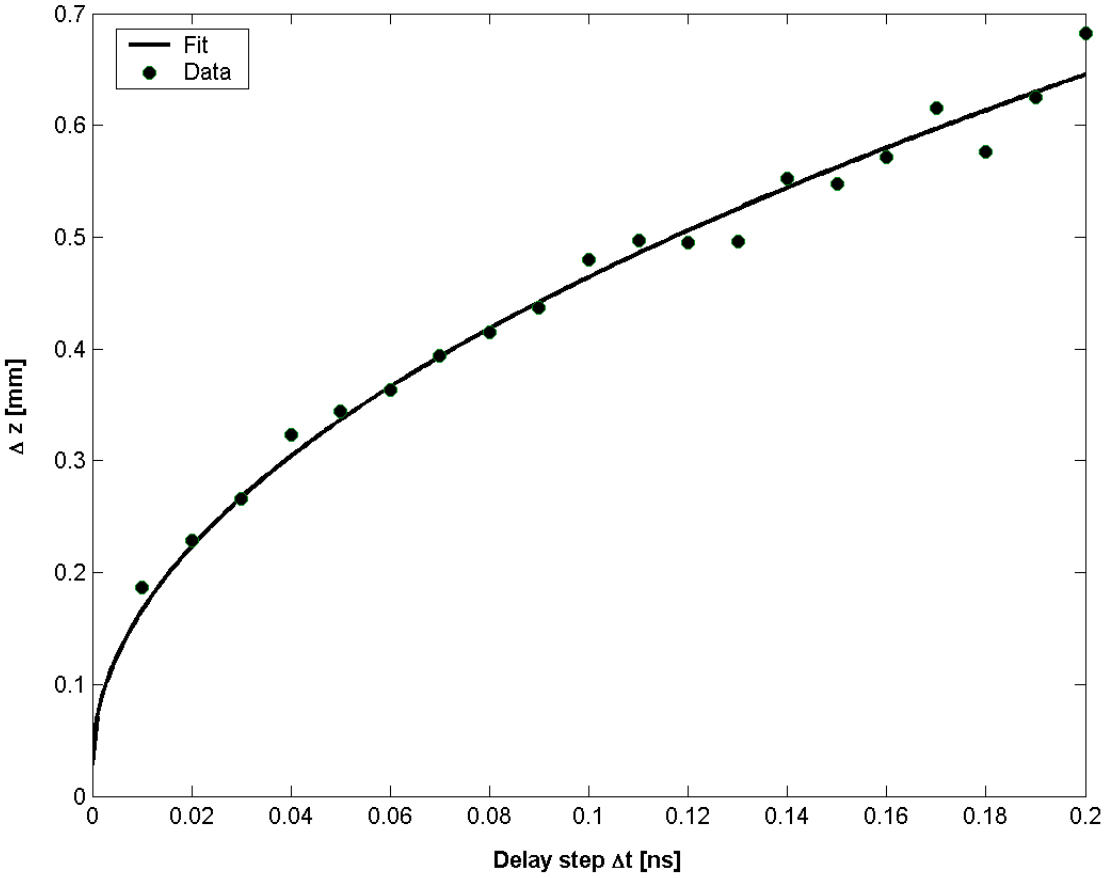

Fig. 4. The distance accuracy Δz vs. delay step size Δt for a gate time t_{gate} =500 *ps*. Dots are measured values and full curve is the prediction of Eq. (5).

The advantage of our system is that the timing accuracy inherent in σ is a system parameter depending only on the laser pulse width and the camera gate time. It is therefore independent of the range[1] to first approximation, and does not get worse at long ranges as do, e.g., triangulation methods. The *SNR* does generally decrease with increasing range for our system because we have to increase the camera gain. We can partly compensate by using larger optics (smaller field-of-view) or decreasing the field of illumination. Therefore, the system accuracy Δz remains small even at longer distances. The real limitations to our technique are found to be turbulence, vibrations of the telescope, drift in laser-to-camera triggering, etc. The resulting total distance accuracy for our system therefore increases gradually to $\Delta z \sim 1$ *mm* at a range of 500 *m*.

[1] By "range", we mean the average distance z over the target pixel's in the image sequence.

4. Space Shuttle inspection in 3-D

To demonstrate the capabilities and accuracy of our system we have recorded 3-D images of standard Lego blocks and a Lego model of the Discovery Space Shuttle. The sizes and standards of Lego blocks are well known and have the right size to illustrate the high accuracy of our 3-D laser radar system.

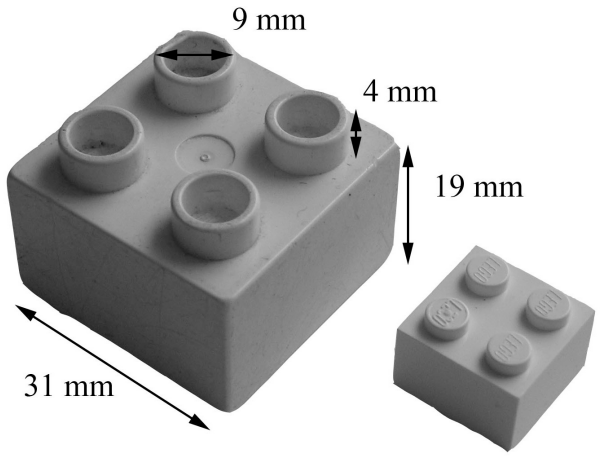

Fig. 5. Left: Dimensions of the Duplo-block. Right: The Lego-block is half the size of the Duplo-block in all dimensions.

To demonstrate the distance accuracy we have recorded images of a simpler target as shown in Figs. 6-7. The target is four rows of Duplo blocks each of height 19 *mm* on a background plate. The Duplo blocks are of different color and reflectivity. A Duplo- and a Lego-block are shown in Fig. 5. Fig. 7 shows the distance vs. pixels in the x-direction at a range of approximately 8 *m* and 200 *m*. At 8 *m* range, the distance accuracy is submillimeter in each pixel as described above. Note that the background distance curves slightly as $\sim\sqrt{(r^2+x^2)}$, where r is the range. The same target is observed at a range of approximately 200 *m*. The images are recorded as at 8 m, however, with a 14-inch Celestron telescope with a focal length of 4 *m*. The Dublo blocks can still be resolved with a distance accuracy of ~1 mm. However, significant smearing takes place over the pixels in the x- (and y-) direction. The smearing is mainly caused by turbulence and vibrations. Turbulence occurs not only at the target but in our case also at the wide opening of our telescope. In space turbulence is absent as well as other medium disturbances, e.g. medium scattering, etc. Due to the large focal length and small field-of-view of the telescope, it is very sensitive to small vibrations. One must therefore use a platform for the camera where vibrations are damped such that the smearing in (*x,y*) pixels can be reduced effectively.

The conclusion from these images is that the 3-D accuracy is in air not limited by the distance resolution but by smearing in (*x,y*) directions due to turbulence and vibrations which can be eliminated in space. We therefore expect submillimeter accuracy in 3-D for our laser radar system in space at ranges up to several hundred meters.

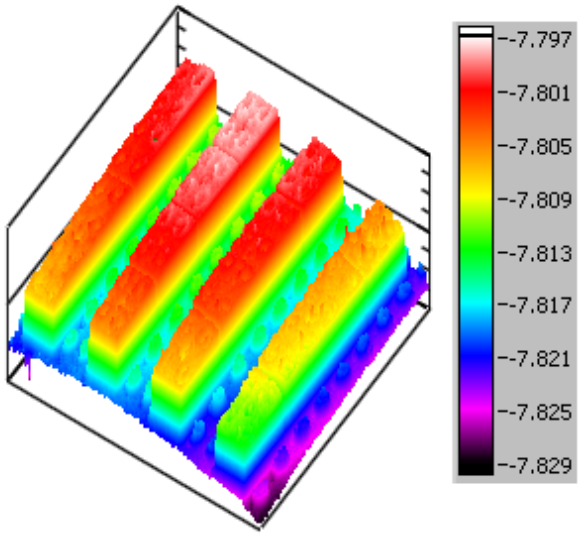

Fig. 6. Range image of 4 rows of Duplo-blocks. The color scale is in meters.

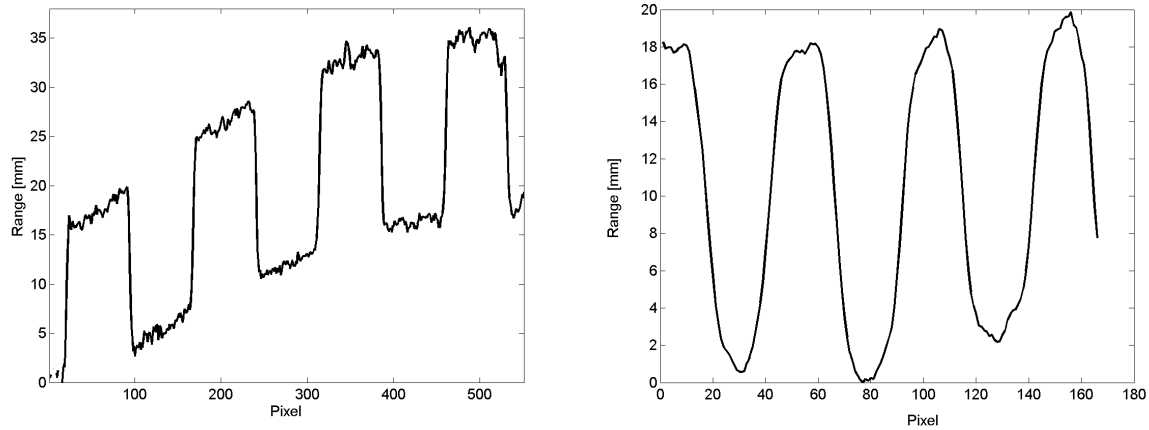

Fig. 7. Distance $z(x,y)$ vs. pixels in the x-direction for fixed y. The ranges are 8 *m* at left and 200 *m* at right (the scales have been subtracted 8 *m* and 200 *m* respectively). The curvature $\sim\sqrt{(r^2+x^2)}$ is obvious at the short range $r = 8$ *m*. The distance accuracy in z is submillimeter at 8 *m* range and ~1 *mm* at 200 *m*. Smearing over pixels in the x- (and y-) directions is observed at 200 *m* range due to turbulence and vibrations as discussed in the text.

In Fig. 8, we show 2-D and 3-D images of a Lego model of the Discovery Space Shuttle.
The Discovery was in operation in July 2005 where it was docking at the ISS. The 40 *cm* x 27 *cm* model of the Discovery is build of white and black Lego blocks of various sizes. Fig. 8 shows the 2-D reflectance image on top and below the corresponding 3-D image is shown. The images are taken at an average range of approximately 8 *m* by a series of 100 frames with a delay step of 10 *ps* and 500 *mm* optics.

Fig. 8. Laser radar images of a 40 *cm* x 27 *cm* Lego model of a space shuttle taken at a range of 8 *m* with our system. The 2-D intensity image $I(x,y)$ is shown on top whereas the range image $z(x,y)$ with color scaling is shown below. The insert is a zoom of the cargo bay demonstrating the <1mm depth accuracy of the small Lego blocks at the right of Fig. 5.

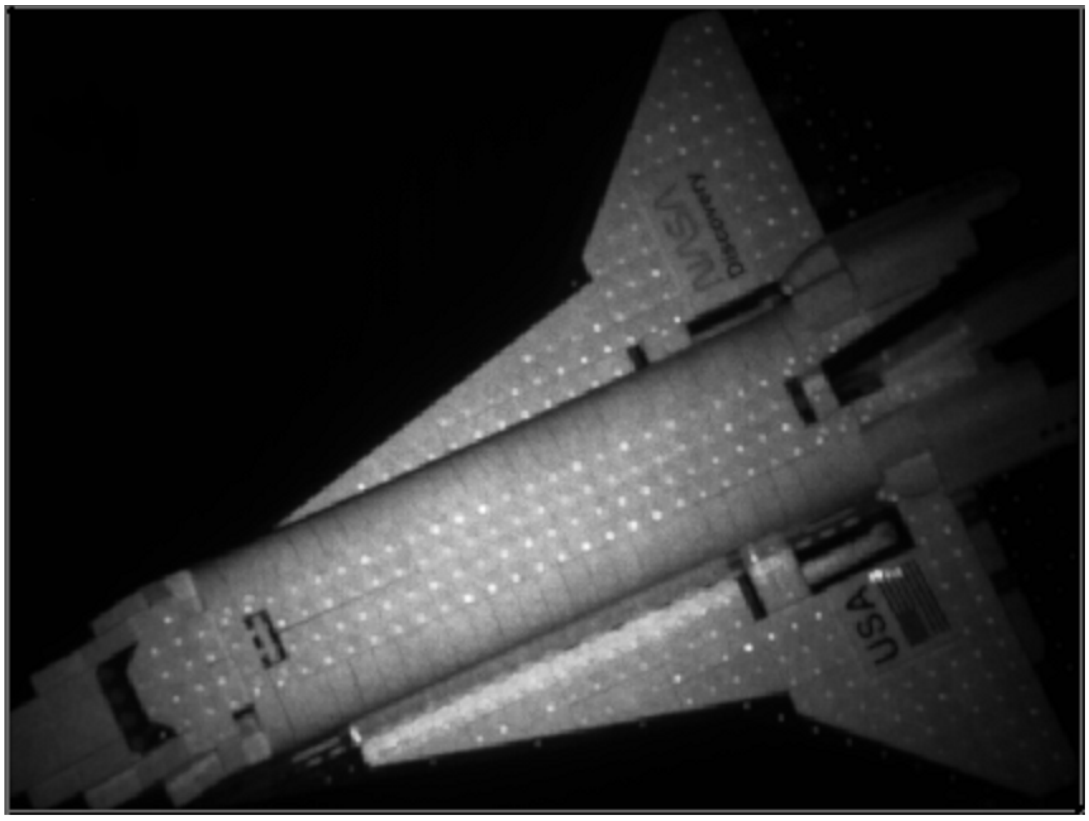
NASA
USA

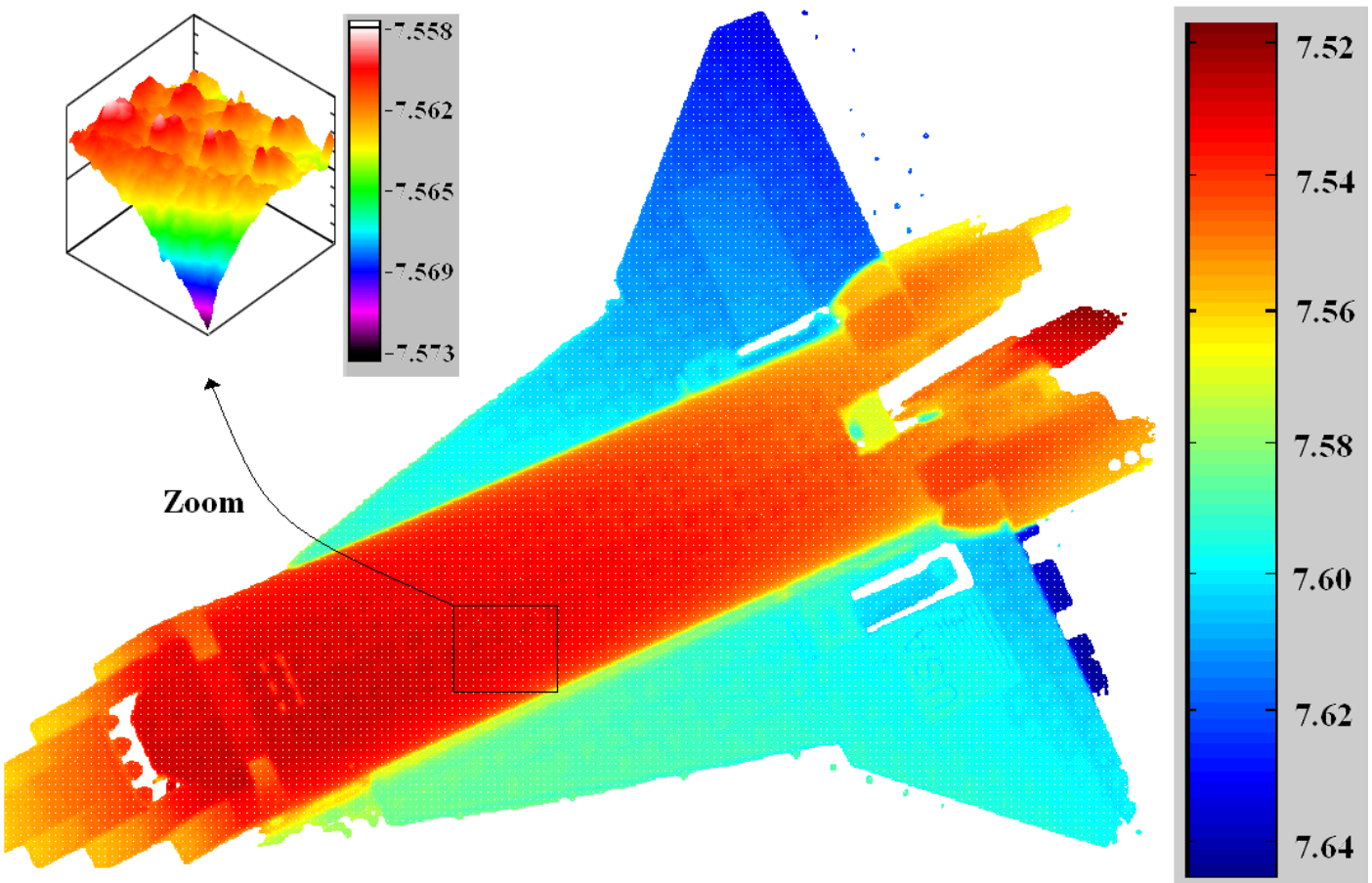
-7.558
-7.562
-7.565
-7.569
-7.573
Zoom
7.52
7.54
7.56
7.58
7.60
7.62
7.64

The model is on scale ~1:100. To cover a real size space shuttle with the same 3-D accuracy will require many such 3-D images. If the optics is chosen such that the target is covered by a few pixels per millimeter, then one image will cover only ~0.1 m^2. It will then take a few thousand 3-D images to cover the whole thermal protection shield of the space shuttle. As each 3-D image takes a few seconds to record, the high accuracy scan will take about an hour. A larger 3-D image can be constructed by an image-mosaic algorithm that combines the individual high accuracy range images.
The algorithm should correct for possible curvatures as, e.g., seen in Fig. 7. The 3-D image can then be utilized for automated tile inspection. Alternatively, a faster scan with lower resolution may be performed where one subsequently can zoom in on tiles suspect of damage.

5. Summary and outlook

It has been demonstrated that our laser radar system can take high accuracy 3-D images at short and long distances up to several hundred meters. The technology can be pressed to take 3-D images down to an accuracy of 0.2 *mm* at ranges up to ~20 *m*. At larger ranges less laser light is returned requiring higher gain. The resulting poorer *SNR* leads to a distance accuracy of 1-2 *mm* around 200 *m* range. For low reflectivity dark tiles, a more powerful laser may therefore be required at long distances in order to retain the high distance accuracy.

In space turbulence is absent. The platform should be chosen with care in order to reduce and damp vibrations for imaging at long distances otherwise smearing in the (x,y) pixels takes place. In the absence of turbulence and vibrations we expect that our system can achieve a submillimeter accuracy in all three (x,y,z) directions of most targets at short distances as well as up to ranges of a few hundred meters.

The pulsed green laser is generally not eye-safe at short distances and astronauts must take care of the beam. The laser is, however, eye-safe at ranges beyond 60 *m* due to its beam divergence and limited power. At short distances the beam is spread out to cover a larger field-of-illumination and is therefore also eye-safe at ~8 *m*.

The high accuracy laser radar system described here is compact, scanner free, speckle free, fast and simple to use. It is therefore very suitable for accurate 3-D imaging of, e.g., surface tiles of space shuttles, as well as other applications requiring high 3-D accuracy.

REFERENCES

1. J. Lamoreux, J. Siekierski, and J. P. N. Carter, “Space shuttle thermal protection system inspection by 3D imaging laser radar”, Proc. SPIE, **5412**, 273-281, 2004.
2. D. Gregoris, A. Ulitsky, D. Vit, A. Kerr, P. Dorcas, G. Bailak, J. Tripp, R. Gillett, C. Woodland, R. Richards, and C. Sallaberger, “Laser imaging sensor system for on-orbit shuttle inspection”, Proc. SPIE, **5418**, 61-68, 2004
3. A. M. DesLauriers, I. Showalter, A. Montpool, R. Taylor, and I. Christie, “Shuttle TPS inspection using triangulation scanning technology”, Proc. SPIE, **5798**, 26-33, 2005.
4. R. Gillett, E. Martin, and A. Ulitsky, “I-SIL: Features, characteristics and capabilities of a long range shuttle inspection lidar system”, Proc. SPIE, **5798**, 34-43, 2005.
5. O. Steinvall, L. Klasen, C. Grönvall, U. Söderman, S. Ahlberg, Å. Person, M. Elmqvist, H. Larsson, D. Letalick, P. Andersson, T. Carlsson, and M. Henriksson, “3D laser sensing at FOI – overview and a system perspective”, Proc. SPIE, **5412**, 294-309, 2004.
6. J. Busck and H. Heiselberg, “Gated viewing and high-accuracy three-dimensional laser radar,” *Appl. Opt.*, **43**, 4705-4710, 2004.
7. J.F. Andersen, J. Busck and H. Heiselberg, “Long distance high accuracy 3-D laser radar and person identification” Proc. SPIE, **5791**, 9-16, 2005.
8. D. Gleckler, “Multiple-slit streak tube imaging lidar (MS-STIL) applications”, Proc. SPIE, **4035**, 266-278, 2000.
9. J. W. McLean and J. T. Murray, “Streak-tube lidar allows 3-D ocean surveillance”, *Laser Focus World*, 171-176, Jan. 1998.
10. A. Nevis, R. J. Hilton, S. J. Taylor, B. Cordes, and J. W. McLean, “The advantages of three-dimensional electro-optic imaging sensors”, Proc. SPIE, **5089**, 225-237, 2003.
11. W. Schilling, D. N. Barr, G. C. Templeton, L. J. Mizerka, and C. W. Trussel, “Multiple-return laser radar for three-dimensional imaging through obscurations”, *Appl. opt.*, **41**, 2791-2799, 2002.
12. M. A. Albota, R. M. Heinrichs, D. G. Kocher, D. G. Fouche, B. E. Player, M. E. O’Brien, B. F. Aull, J. J. Zayhowski, J. Mooney, B. C. Willard, and R. R. Carlson, “Three-dimensional imaging laser radar with a photon-counting avalanche photodiode array and microchip laser”, *Appl. Opt.*, **41**, 7671-7678, 2002.
13. R. Lange and P. Seitz, “Seeing distances – a fast time-of-flight 3D camera”, *Sensor Review*, **20**, 212-217, 2000.
14. K. Aliberti et al., “Characterizaton of InGaAs self-mixing detectors for chirp, amplitude-modulated LADAR, Proc. SPIE, **4377**, 99-110, 2001.
15. R. Stettner, H. Bailey, and R. Richmond, “Eye-safe laser radar 3-D imaging”, Proc. SPIE, **5412**, 111-116, 2004.
16. G. S. Cheok and W. C. Stone, “Performance evaluation facility for LADARS”, Proc. SPIE, **5412**, 54-65, 2004.
17. J. Busck, “Underwater three-dimensional optical imaging with a gated viewing laser radar”, to appear in *Opt. Eng*., 2005.